DOI:10.1093/jnci/djs319
Advance Access publication on August 21, 2012.

ARTICLE

Effect of Inhibition of the Lysophosphatidic Acid Receptor 1 on Metastasis and Metastatic Dormancy in Breast Cancer

Jean-Claude A. Marshall, Joshua W. Collins, Joji Nakayama, Christine E. Horak, David J. Liewehr, Seth M. Steinberg, Mary Albaugh, Fernando Vidal-Vanaclocha, Diane Palmieri, Maryse Barbier, Maximilien Murone, Patricia S. Steeg

Manuscript received August 10, 2011; revised June 13, 2012; accepted June 18, 2012.

Correspondence to: Patricia S. Steeg, PhD, Bldg 37, Rm 1122, National Institutes of Health, Bethesda, MD 20892 (e-mail: steegp@mail.nih.gov).

Background Previous studies identified the human nonmetastatic gene 23 (*NME1*, hereafter *Nm23-H1*) as the first metastasis suppressor gene. An inverse relationship between *Nm23-H1* and expression of lysophosphatidic acid receptor 1 gene (*LPAR1*, also known as *EDG2* or hereafter *LPA1*) has also been reported. However, the effects of LPA1 inhibition on primary tumor size, metastasis, and metastatic dormancy have not been investigated.

Methods The LPA1 inhibitor Debio-0719 or LPA1 short hairpinned RNA (shRNA) was used. Primary tumor size and metastasis were investigated using the 4T1 spontaneous metastasis mouse model and the MDA-MB-231T experimental metastasis mouse model (n = 13 mice per group). Proliferation and p38 intracellular signaling in tumors and cell lines were determined by immunohistochemistry and western blot to investigate the effects of LPA1 inhibition on metastatic dormancy. An analysis of variance-based two-tailed *t* test was used to determine a statistically significant difference between treatment groups.

Results In the 4T1 spontaneous metastasis mouse model, Debio-0719 inhibited the metastasis of 4T1 cells to the liver (mean = 25.2 liver metastases per histologic section for vehicle-treated mice vs 6.8 for Debio-0719-treated mice, 73.0% reduction, $P < .001$) and lungs (mean = 6.37 lesions per histologic section for vehicle-treated mice vs 0.73 for Debio-0719-treated mice, 88.5% reduction, $P < .001$), with no effect on primary tumor size. Similar results were observed using the MDA-MB-231T experimental pulmonary metastasis mouse model. LPA1 shRNA also inhibited metastasis but did not affect primary tumor size. In 4T1 metastases, but not primary tumors, expression of the proliferative markers Ki67 and pErk was reduced by Debio-0719, and phosphorylation of the p38 stress kinase was increased, indicative of metastatic dormancy.

Conclusion The data identify Debio-0719 as a drug candidate with metastasis suppressor activity, inducing dormancy at secondary tumor sites.

J Natl Cancer Inst 2012;104:1306–1319

Tumor metastasis is a leading contributor to morbidity and mortality in cancer patients. Studies have shown that on reexpression in tumor cell lines, metastasis suppressor genes inhibit metastasis but do not substantially reduce primary tumor size (1–6). The human nonmetastatic gene 23 (*NME1*, hereafter *Nm23-H1*) was the first metastasis suppressor gene identified (7–9), and its functional activity has been confirmed in transfection (9–22) and knockout mouse models (23).

The translation of tumor or metastasis suppressor genes as anticancer therapeutics has been difficult, and identification of targetable proteins with inverse expression patterns as an alternative strategy has been explored in preclinical studies with some success (24,25). Expression of the lysophosphatidic acid receptor 1 gene (*LPAR1*, also known as *EDG2* or hereafter *LPA1*) was inversely associated with expression of *Nm23-H1* in tumor cell lines, human infiltrating ductal breast carcinomas, and liver tumor tissues from wild-type and *Nm23-M1* knockout mice (26). Forced *LPA1* expression in tumor cells with high levels of *Nm23-H1* expression overcame *Nm23-H1*-mediated suppression of motility in vitro (26) and metastasis in vivo (27). Together, these data suggest that a LPA1 inhibitor could act as a metastasis suppressor.

LPA1 is a G-protein-coupled receptor for lysophosphatidic acid (LPA) (28–34), which is present in submillimolar levels in serum (35). LPA1 overexpression in the mammary glands of transgenic mice weakly promoted tumorigenesis (36), but studies have shown that LPA1-mediated signaling also stimulates tumor cell adhesion, motility, invasion, and metastasis (36–43). Multiple inhibitors for LPA1 have been reported (39,44–49), including Debio-0719, a selective stereoisomer of a previously identified Ki16425 LPA1 inhibitor (47). Using both Debio-0719 or short hairpinned RNA (shRNA) to decrease expression of LPA1, we investigated the effects of LPA1 inhibition on metastasis, primary tumor size, and metastatic dormancy using murine 4T1 and human MDA-MB-231T breast carcinoma cell lines in vitro and in vivo.

Methods

Cell Lines

Murine mammary carcinoma 4T1 luciferase-labeled cells, a gift from Dr Gary Sahagian (Tufts University, Boston, MA), were cultured in Dulbecco's modified Eagle medium (DMEM, Invitrogen, Frederick, MD) supplemented with 10% fetal bovine serum. A subline of human MDA-MB-231 cells, designated MDA-MB-231T (50), was generously provided by Dr Zach Howard (Laboratory of Immunoregulation, National Cancer Institute, Bethesda, MD) and was maintained in DMEM supplemented with 10% fetal bovine serum. The MDA-MB-231T cell line was used for its reliable in vivo experimental metastatic potential.

Clones of 4T1 cells expressing flag-tagged Nm23-H1, flag-tagged mouse Nm23 (Nm23-M1), or empty pcDNA3 vector (Invitrogen) were created. The cDNAs were inserted into the BamH1 site in the multiple cloning site of pcDNA3 (Invitrogen), and confirmed by DNA sequencing performed by the National Cancer Institute Core Services (Bethesda, MD). The plasmids were transfected into 4T1 cells using Lipofectamine (Invitrogen, Valencia, CA) by the manufacturer's recommended protocol. Forty-eight hours after transfection, cells were cultured in DMEM containing 10% fetal bovine serum, 600 μg/mL G418 (Invitrogen), and the clonal cell lines were subsequently isolated and cultured.

LPA1 Inhibitors

Debio-0719 was provided by Debiopharm S.A. (Lausanne, Switzerland) and was stored in powder form in the dark at room temperature. For all experiments, Debio-0719 was dissolved into sterile phosphate-buffered saline, and phosphate-buffered saline served as the vehicle control for in vitro and in vivo experiments. For the in vitro assays, Debio-0719 was used at a concentration of 60 nM, which was the half maximal inhibitory concentration for antagonist activity (IC_{50}) (data not shown).

LPA1 knockdown was achieved using two validated lentiviral shRNA constructs from Sigma-Aldrich (St. Louis, MO) as per the manufacturer's recommendations (catalog no. shclnv-nm 010336). Scrambled shRNA constructs were used as a negative control (Sigma-Aldrich).

Western Blots

Whole cell lysates were prepared, and protein concentrations were determined using the methods given in the Supplementary Materials (available online). After proteins were separated by sodium dodecyl sulfate polyacrylamide gel electrophoresis and transferred to nitrocellulose membranes, the membranes were probed with antibodies and then visualized on X-ray film (Supplementary Methods and Supplementary Table 1, available online).

In Vitro Functional Assays

Cell proliferation was measured by 3-(4,5 dimethylthiazol-2-yl)-2,5-diphenyltetrazolium bromide (MTT) assay (Supplementary Methods, available online). Anchorage-independent growth was also assessed (Supplementary Methods, available online). For both the cell proliferation and anchorage-independent growth assays, five independent experiments were performed.

Migration assays were performed as described [(26) and Supplementary Methods, available online]. Briefly, 4T1 or MDA-MB-231T cells were incubated in the top compartments of Boyden chambers in the presence of vehicle control or varying concentrations of Debio-0719. The number of cells that had migrated through the chamber was quantified. Three independent experiments were performed, each in triplicate.

Adhesion assays were performed using the CultureCoat Adhesion Protein Array Kit (Trevigen, Gaithersburg, MD) as per the manufacturer's recommended protocol (Supplementary Methods, available online).

In Vivo Studies

All mouse experiments were performed under an approved National Cancer Institute Animal Use Agreement. Female six-week-old Balb/c or athymic NRC nu/nu mice were used.

Spontaneous Metastasis Mouse Model. For the spontaneous metastasis experiments, 4T1 cells (parental or modified by stable transfection with one of two LPA1 shRNAs, a scrambled shRNA, Nm23-H1 constructs, or a vector control construct) were injected into the mammary fat pads of female Balb/c mice (n = 10 mice per group) (Supplementary Methods, available online). The primary tumors were measured twice weekly until resection, which occurred on days 10 or 14, depending on the experiment. After 8–11 weeks, depending on the experiment, all lymph nodes, lungs, livers, and any other organ suspected of harboring a metastasis were collected for histologic analysis. The schedule of randomization to vehicle (phosphate-buffered saline) or Debio-0719 (15 mg/kg given subcutaneously twice daily) varied by experiment (Supplementary Methods, available online). Drug treatment started on day 2 postinjection of cells for efficacy experiments and on day 15 postinjection of cells for adjuvant experiments.

Experimental Pulmonary Metastasis Mouse Model. To investigate the effect of LPA1 inhibition on metastasis of human breast cancer cells in vivo, an experimental pulmonary metastasis study was conducted. Athymic NRC nu/nu mice were injected with 5×10^5 MDA-MB-231T human breast cancer cells via the tail vein [(50) and Supplementary Methods, available online]. On the day following injection, mice were randomized into three groups containing 13 mice each. The mice were assigned to one of the following treatment groups: vehicle, 15 mg/kg Debio-0719 given twice daily subcutaneously or 15mg/kg Debio-0719 given twice daily subcutaneously for 35 days followed by administration of vehicle control for the remainder of the study. Mice were killed at day 42 by being placed in a carbon dioxide chamber, and the lungs were collected and fixed in Bouins' solution (50). Surface metastatic lesions were counted on all lungs using a magnifying glass, blinded to the treatment group, before the lungs were embedded in paraffin for histological analysis (Supplementary Methods, available online).

To investigate the effect of LPA1 inhibition on primary tumor growth, 5×10^5 MDA-MB-231T human breast cancer cells were implanted into the mammary fat pads of athymic NRC nu/nu mice. The day following implantation, mice were randomized into two groups of five mice each and treated with vehicle control or 15 mg/kg Debio-0719 given twice daily subcutaneously. The growth of

the primary tumor in the mammary fat pad was measured twice weekly by caliper until day 32, at which time they were killed in a carbon dioxide chamber. The tumors were then excised, and 5-μm sections were stained with hematoxylin and eosin and analyzed by a pathologist. Tissues were also used for immunofluorescence or immunohistochemical staining (51) for expression of different proteins (Supplementary Methods, available online).

Primary Organ–Conditioned Media

Conditioned medium collected from primary cultures of mammary fat pads, livers, and lungs from Balb/c mice (Supplementary Methods, available online) was assayed for soluble cytokine expression using cytokine antibody arrays per the manufacturer's protocol (Supplementary Methods, available online).

To model activation of Erk and p38 in vitro, 4T1 cells that were plated on type I collagen-coated 35-mm dishes were cultured in the presence of vehicle or Debio-0719 for 48 hours and then serum-starved overnight. To study activation of phosphorylated proteins (Erk and p38) or total protein levels (MKKK1, MKK3, MKK4, MKK6, and p27), cells were then stimulated with 20% (v/v) conditioned medium from mammary fat pads, livers, or lungs before lysis and western blot analysis.

Statistical Analysis

A variety of analyses of variances (ANOVA) were performed on the raw or transformed data. Please see the Supplementary Methods (available online) for details. A nonparametric Wilcoxon rank sum test was used to compare distributions if the data were not normally distributed and/or the sample sizes were less than 10 mice per group. Dunnett method was used to adjust the *P* values for pair-wise comparisons between a control and other treatment. Otherwise, Holm method was used to adjust pair-wise *P* values. Because of the multiple tests, we consider a *P* of .01 as the upper limit of what may be interpreted as being statistically significant; a strong trend was indicated if *P* was greater than .01 but less than .05, and any *P* greater than .05 was not statistically significant. Diffuse metastasis counts, in which metastases filled the liver and quantitative counts were not feasible, were excluded from the statistical analysis because they could potentially introduce bias. Actuarial analyses were performed on the survival data using the Kaplan–Meier method, and curves were compared using the log-rank test. Survival times were censored if the mouse was alive at the time of the last follow-up. All *P* values were two-sided.

Results

Nm23-H1 Function in a 4T1 Metastasis Model System

Luciferase-expressing 4T1 murine mammary carcinoma cells produce primary orthotopic mammary tumors and widespread spontaneous metastases in immunocompetent mice (52). qRT-PCR of 4T1 cells demonstrated expression of LPA family receptors LPA1, LPA2, LPA6, and related GPR87, with minor expression of LPA3, LPA4, LPA5, and related P2Y10 (data not shown). To determine the effect of Nm23 overexpression, 4T1 cells were transfected with a vector construct (VC), or the human (H1) or murine (M1) homologs of Nm23 (Figure 1, A). Mammary fat pad primary tumor sizes from clonal lines at the time of resection were comparable between Nm23 and vector transfectants (Figure 1, B). Overexpression of Nm23 reduced the number of metastases to the liver by 62.4%–69.7% and lungs by 85.1%–94.6% (all $P < .05$ compared with either 4T1 parental or vector controls) (Figure 1, C and D). Expression of LPA1 was reduced in 4T1 cells and primary tumors overexpressing Nm23 (Figure 1, E and F).

The molecular structure of Debio-0719, an LPA1 inhibitor, is shown (Figure 2, A). The half maximal inhibitory concentration for antagonist activity of Debio-0719 for LPA1 was 60 nM, with less potent inhibition of LPA3 at 660 nM and LPA2 at 2 μM (data not shown). In vitro, Debio-0719 exerted little antiproliferative effect on 4T1 cells (data not shown) but inhibited their motility (Supplementary Figure 1, available online).

4T1 Spontaneous Metastasis Experiments Using Debio-0719

Figure 2, B outlines the first set of 4T1 experiments to test the hypothesis that a LPA1 inhibitor would act as a metastasis suppressor. Mice were injected with 4T1 cells in the mammary fat pads on day 0 and then randomized to vehicle or Debio-0719 beginning 2 days postinjection. Mice injected with an Nm23-M1 transfectant of 4T1 cells and treated with vehicle served as a positive control for metastasis suppressor activity. No antitumor effect of Debio-0719 was observed in the primary tumors at the time of resection on day 10 postinjection ($P = .98$) (Figure 2, C and D). Therefore, this compound would not normally be further studied for drug development purposes.

Imaging experiments to determine 4T1 metastatic burden, conducted on day 70 postinjection, showed that Debio-0719 had a metastasis-suppressive effect (Figure 2, D). Enlarged lymph nodes were apparent at the time of necropsy in 22 (55.0%) of 40 vehicle-treated mice vs 6 (15.0%) of 40 Debio-0719-treated mice and 6 (15.0%) of 40 mice with 4T1 Nm23-M1a tumors in which metastasis was suppressed. A mean of 25.2 liver metastases per histologic section was observed for vehicle-treated mice vs 6.8 for Debio-0719-treated mice (73.0% reduction, median difference = 18.4 metastases per liver, 95% confidence interval [CI] = 12.7 to 24.2, $P < .001$) and 5.3 for mice injected with 4T1 Nm23-M1a cells (79.0% reduction, median difference = 19.9 metastases per liver, 95% CI = 16.2 to 23.7, $P < .001$) (Figure 2, E). In addition, 6 (15.0%) of 40 vehicle-treated mice exhibited diffuse sinusoidal liver metastasis that could not be quantified (Supplementary Figure 2, available online) vs 3 (7.5%) of 40 mice treated with Debio-0719. The mice with diffuse metastases were not included in the statistical analysis and therefore represent a potential bias because they would all reflect large values. A similar trend was observed in lung metastases when a mean of 6.37 lesions per histologic section was observed for vehicle-treated mice vs 0.73 lesions per section for Debio-0719-treated mice (88.5% reduction, median difference = 5.64 metastases per lung, 95% CI = 4.75 to 6.53, $P < .001$) and a 90.1% decline to 0.63 lesions per section for mice injected with 4T1 Nm23-M1a, vehicle-treated cells (median difference = 5.74 metastases per lung, 95% CI = 4.87 to 6.61, $P < .001$) (Figure 2, E and Supplementary Figure 2, available online). The number of lung metastases produced by 4T1 Nm23-M1a transfectants was not statistically significantly different from those produced by 4T1 cells treated with Debio-0719 ($P = .72$). Debio-0719

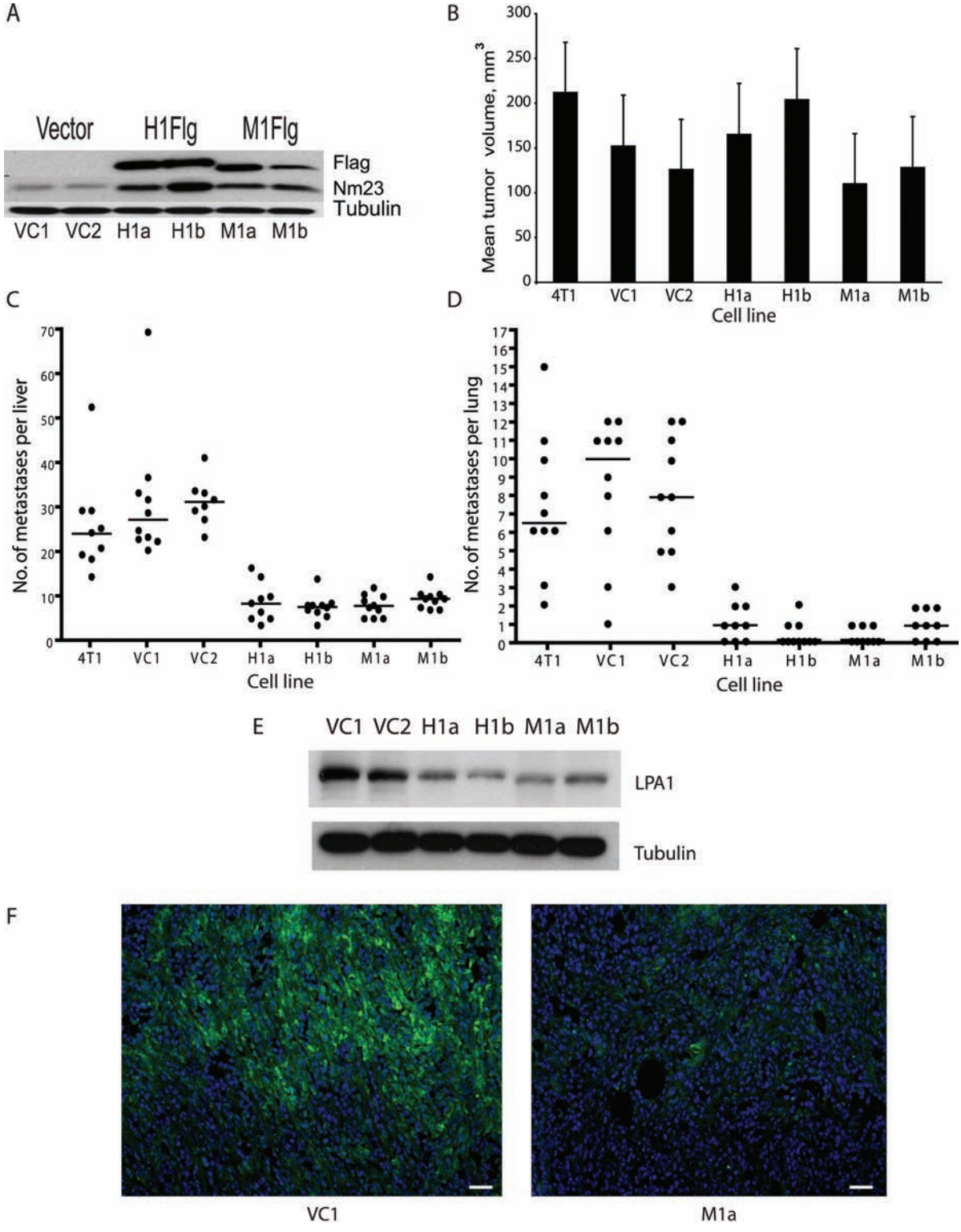

Figure 1. Effects of nonmetastatic gene 23 (Nm23) suppression on metastasis and lysophosphatidic acid receptor 1 (LPA1) expression in the 4T1 spontaneous metastasis mouse model. **A**) Nm23 expression in independent clones of 4T1 murine mammary cells transfected with either a vector construct (VC1 and VC2), flag-tagged Nm23-H1 (human ortholog, H1Flg construct; H1a and H1b clones) or flag-tagged Nm23-M1 (mouse ortholog, M1Flg construct; M1a and M1b clones) was confirmed by western blot. Tubulin was used as the loading control. **B**) The size of primary tumors in the mammary fat pad formed by the parental 4T1 cell line and each clone on day 10 postinjection (n = 20 Balb/c mice per group) was measured. The least-squares mean tumor volume and 95% confidence intervals (**whisker bars**) are shown. The mean number of metastases in the (**C**) liver and (**D**) lungs (**bar**) was determined at day 70 after orthotopic injection. Metastases were quantified from step sections of tissues stained with hematoxylin and eosin. The combined results from two independent experiments are presented. **E**) Western blot analysis of LPA1 protein expression in the transfected clones is shown. Tubulin was used as the loading control. **F**) The primary tumors from mice injected with the VC1 and M1a clones sectioned and underwent immunofluorescence staining for LPA1 protein (**green**). Tumor nuclei were stained with 4′,6-diamidino-2-phenylindole (DAPI, **blue**). Scale bar = 220 μm.

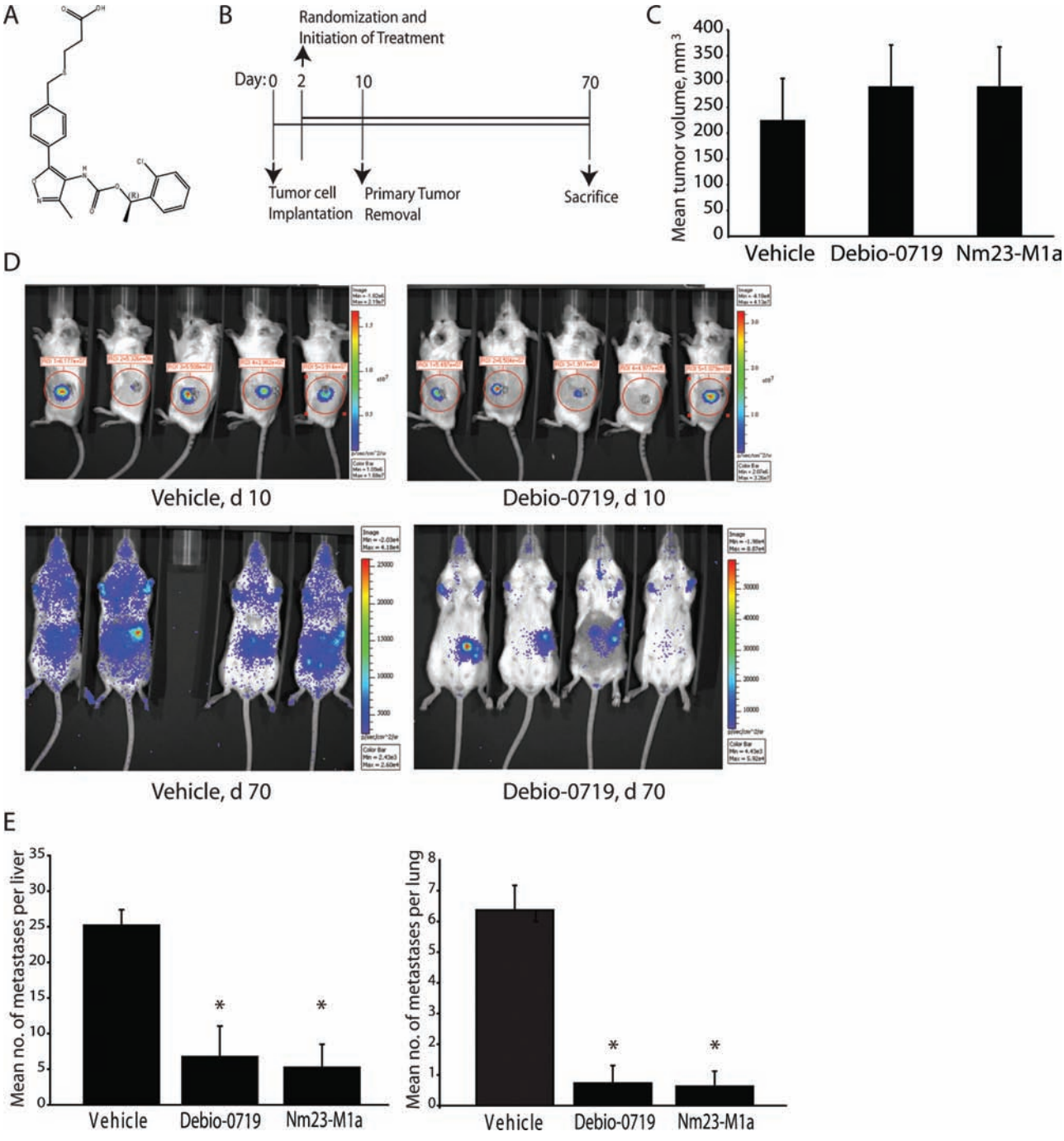

Figure 2. The effect of treatment with Debio-0719 on metastasis suppression in the 4T1 spontaneous metastasis mouse model. **A**) The chemical structure of Debio-0719 is depicted. **B**) The experimental design is outlined. 4T1 cells were injected into the mammary fat pads of Balb/c syngeneic mice on day 0. On day 2, mice were randomized to receive vehicle or 15 mg/kg Debio-0719 given subcutaneously twice daily. Primary tumors were resected on day 10 postinjection. Mice were killed on day 70 postinjection, and the metastases were quantified. Combined data from two independent experiments are shown (n = 40 mice per group). A third experimental group of 4T1 cells transfected with mouse nonmetastatic gene 23 (Nm23-M1; hereafter M1a cells) was treated with vehicle (n = 40) as a positive control. **C**) The least-squares mean of the primary tumor size and corresponding 95% confidence intervals (**whisker bars**) at day 10 postinjection are given. **D**) Representative images of primary tumors on day 10 postinjection (left panels) and metastatic burden on day 70 postinjection (right panels) taken using a Xenogen In Vivo Imaging System (Caliper Life Sciences, Hopkinton, MA) are shown. Please see the color scale to the right of each image, which shows the intensity range of photon flux per second from the 4T1 cells. **E**) The mean number of metastases in step sections of liver and lungs and 95% confidence intervals (**whisker bars**) are shown. *P <.001 compared with the vehicle control-treated mice and was determined by a two-sided t test done with transformed data. The differences between the mean number of metastases to the liver for Debio-0719 and M1a vehicle-treated groups were not statistically significant. Similar results were seen for metastases to the lungs.

was reliably detected in serum, and the weight measurements of mice indicated no overt toxic effects (Supplementary Figure 3, available online).

To confirm that LPA1 inhibition was responsible for metastatic suppression, LPA1 expression in 4T1 cells was stably knocked down using shRNAs (Figure 3, A). Knockdown of LPA1 expression by

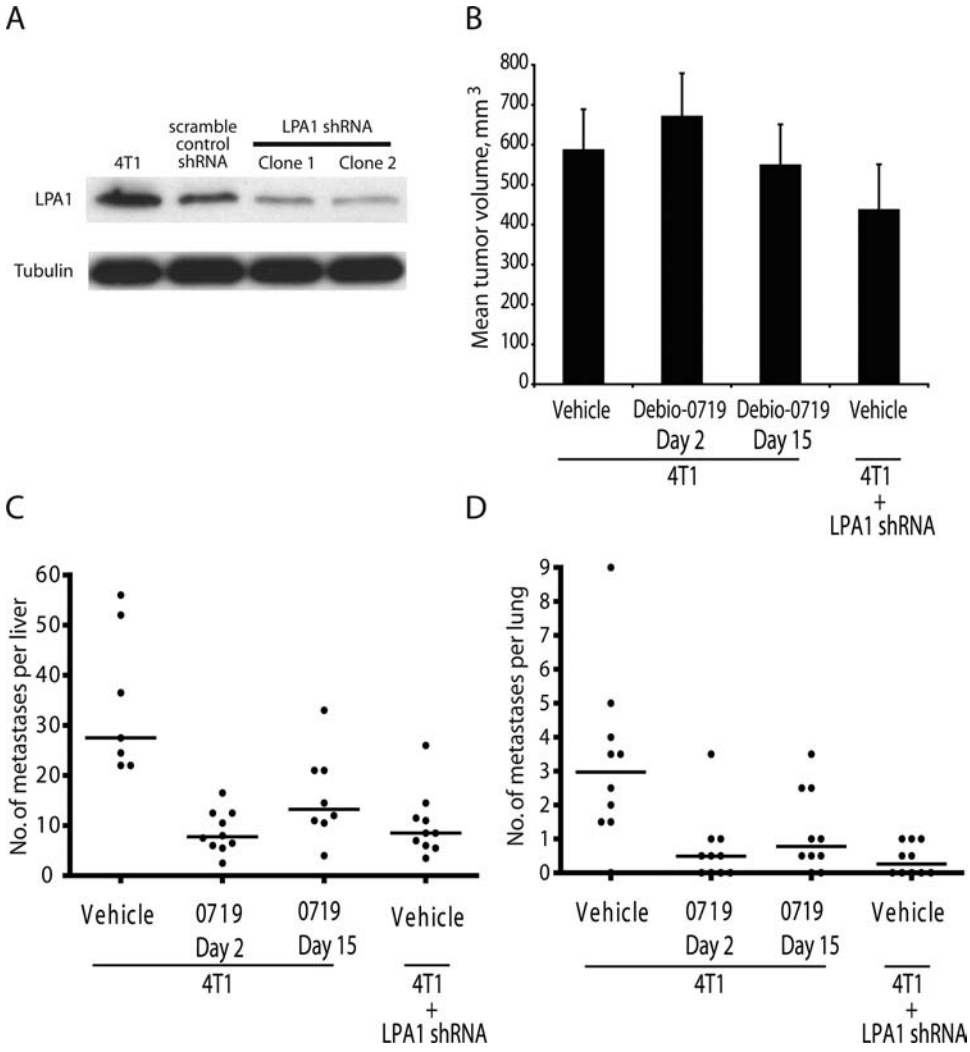

Figure 3. Effect of treatment with Debio-0719 on metastasis in the 4T1 spontaneous metastasis mouse model. **A**) 4T1 cells were transfected with a scramble control short hairpinned RNA (shRNA) or one of two independent shRNAs targeting lysophosphatidic acid receptor 1 (LPA1; clone 1 and clone 2). Cell lysates were collected and underwent western blot for LPA1. Tubulin was used as the loading control. **B–D**) Syngeneic Balb/c mice were injected with 4T1 cells into the mammary fat pad on day 0, and primary tumors were resected on day 14 postinjection. The mice were randomized to vehicle (n = 10) or 15 mg/kg of Debio-0719 subcutaneously administered twice daily (n = 10) beginning either on days 2 or 15 postinjection. The 4T1 LPA1 shRNA clone 1 was also injected and treated with vehicle as a positive control (n = 10). **B**) Primary tumor size was measured, and the least-squares mean and 95% confidence intervals (**whisker bars**) are shown. **C–D**) The mean number of metastases (**bar**) in the liver and lungs per histologic section on day 56 postinjection was determined.

Table 1. Effect of LPA1 knockdown in a 4T1 mammary carcinoma spontaneous metastasis model*

	Scrambled shRNA		LPA1 shRNA		
Response	**Vehicle (n = 10)**	**Debio-0179 (n = 9)**	**Vehicle (n = 10)**	**Debio-0179 (n = 10)**	***P***
Least-squares mean tumor size, mm^3 (95% CI)	400 (290 to 510)	336 (226 to 446)	356 (249 to 469)	357 (247 to 467)	.86
No. of mice with diffuse liver metastases	3	1	1	0	–
Median no. of liver metastases per section (95% CI)	24 (19 to 101)	6.25 (2.5 to 13)	13.5 (8.5 to 20)	5.75 (4.0 to 8.0)	.01
% relative to control	100	26.0	56.3	24.0	
Median no. of lung metastases per section (95% CI)	2.0 (1.5 to 3.5)	0.5 (0 to 1.5)	1.0 (0 to 1.0)	0 (0 to 1.0)	.004
% relative to control	100	25.0	50.0	0	

* 4T1 murine mammary carcinoma cells were transfected with a scrambled or LPA1 shRNA. Transfectants were injected into the mammary fat pads of syngeneic Balb/c mice and after 2 days, mice were randomized to vehicle (phosphate buffered saline) or 15 mg/kg Debio-0719 administered subcutaneously twice daily. The size of the primary tumor was measured using calipers on day 14 postinjection, and the primary tumor was resected. The metastases were quantified at day 56 postinjection. CI = confidence interval; LPA1 = lysophosphatidic acid receptor 1; shRNA = short hairpinned RNA.

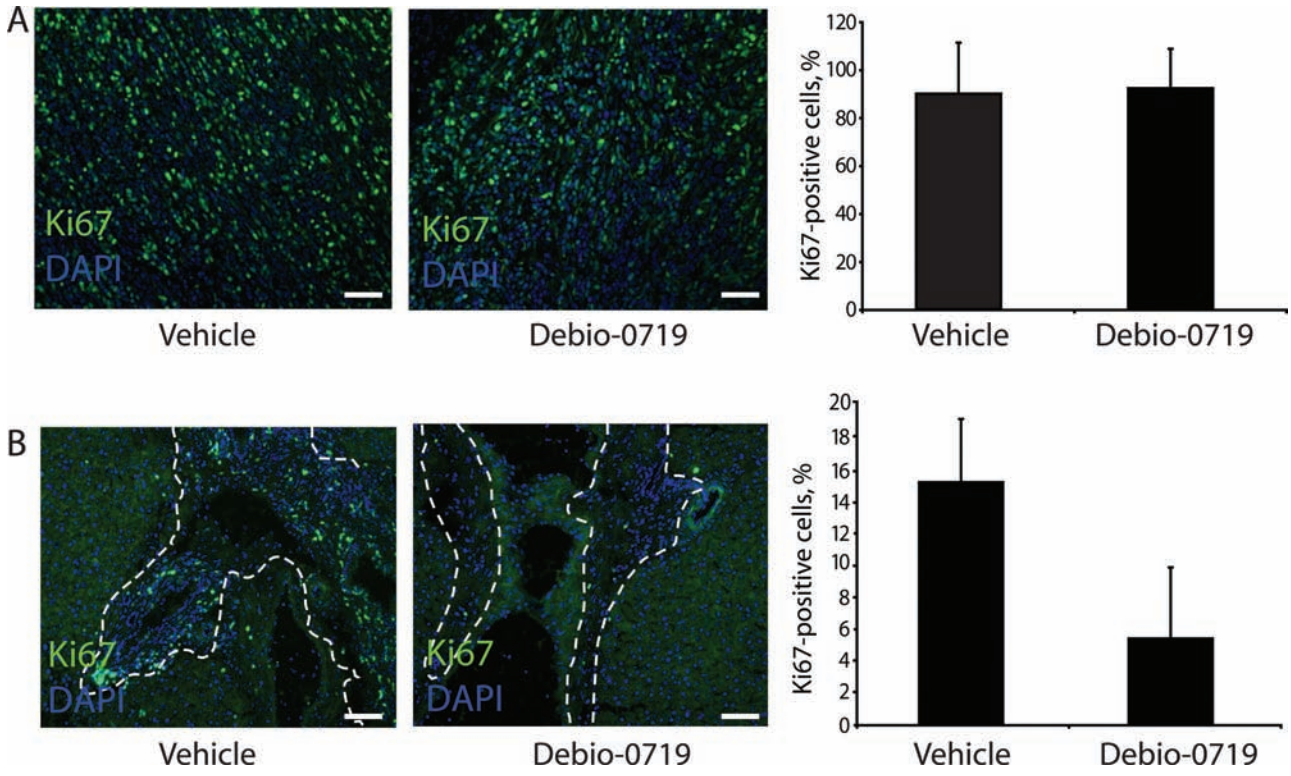

Figure 4. Effect of treatment with Debio-0719 on tumor proliferation in the 4T1 spontaneous metastasis mouse model. The primary tumor and liver and lung tissues from the mice used in experiments described in Figure 2, B–E were analyzed for Ki67 as a marker of dormancy. Tissue sections from the (**A**) primary tumors and (**B**) metastases in the liver (indicated by **white dotted lines**) from mice injected with 4T1 cells and treated with either vehicle control or Debio-0719 (15 mg/kg administered subcutaneously twice daily) underwent immunofluorescence staining for Ki67 (**green**). Tumor nuclei were stained with 4′,6-diamidino-2-phenylindole (DAPI, **blue**). The mean expression levels of Ki67 (n = 5 mice per group) were determined and were calculated as the mean ratio of Ki67 to DAPI. Corresponding 95% confidence intervals are indicated by the **whisker bars**. Representative images are shown. *P =.005 compared with the vehicle control-treated mice and was determined by a two-sided t test. Scale bar = 220 μm.

shRNA decreased the in vitro motility of 4T1 cells; Debio-0719 did not exhibit an additive or synergistic effect when combined with shRNA to LPA1 (Supplementary Figure 4, available online). An LPA1 shRNA and a scrambled shRNA 4T1 clone were injected into the mammary fat pads of syngeneic mice; on day 2 postinjection, mice in each treatment group were randomized to vehicle or Debio-0719 treatment (Table 1). Mean primary tumor sizes on day 14, just before surgical removal, were similar (P = .86). LPA1 shRNA knockdown reduced liver metastases by 43.7%, from 24 to 13.5 metastases per histologic section (median difference = 10.5 metastases per liver, 95% CI = 4.0 to 22, P = .01), and lung metastases by 50.0%, from 2.0 to 1.0 (median difference = 1.0 metastases per lung, 95% CI = 0.5 to 3.5, P = .004). Thus, LPA1 inhibition mediated metastasis suppression. LPA1 shRNA knockdown showed similiar inhibition of lung metastases, but it was less effective for liver metastases compared with Debio-0719 treatment of mice harboring scrambled shRNA 4T1 cells. Immunoflourescence staining of LPA1 in shRNA 4T1 cell liver metastases demonstrated some reexpression of the target gene in vivo (data not shown), a potential reason for the incomplete effect of LPA1 shRNA in inhibiting metastasis.

Finally, we determined whether the metastasis-suppressive effect of Debio-0719 was independent of treating the primary tumor. An experiment similar in design to that shown in Figure 2, B was conducted, except that primary tumors were removed on day 15 postinjection, and mice were subsequently randomized to vehicle or Debio-0719. Primary tumor size among the randomized groups was comparable (P = .07) (Figure 3, B). Treatment with Debio-0719 beginning on day 15 postinjection reduced the number of liver metastases per histologic section at necropsy on day 56 postinjection by 51.6% from 27.5 to 13.3 (median difference = 14.2 metastases per liver, 95% CI = 3.5 to 40.5, P = .01) (Figure 3, C) and the number of lung metastases per section by 75.0% from 3.0 to 0.75 (median difference = 2.3 metastases per lung, 95% CI = 0 to 3.5, P = .11) (Figure 3, D). These metastatic burdens were not statistically significantly different from either Debio-0719 administered beginning on day 2 postinjection or 4T1 cells expressing an LPA1 shRNA and treated with vehicle (P = .61 and .41, respectively). Taken together, LPA1 inhibition, by shRNA or Debio-0719, has antimetastatic function in the 4T1 model system.

LPA1-Mediated Metastasis Suppression Exhibits Hallmarks of Dormancy

Histologic sections of primary and metastatic 4T1 tissues were analyzed for proliferative and apoptotic markers to determine the mechanism of site-specific responsiveness to Debio-0719. The Ki67 labeling of primary tumors from mice treated with vehicle or Debio-0719 was comparable (P = .86) (Figure 4, A). In contrast, in vehicle-treated liver metastases, 15.3% of tumor cells were Ki67 positive and declined by 64.7% to 5.4% in the Debio-0719-treated lesions (median difference = 9.9% of cells positive, 95% CI = 4.1%

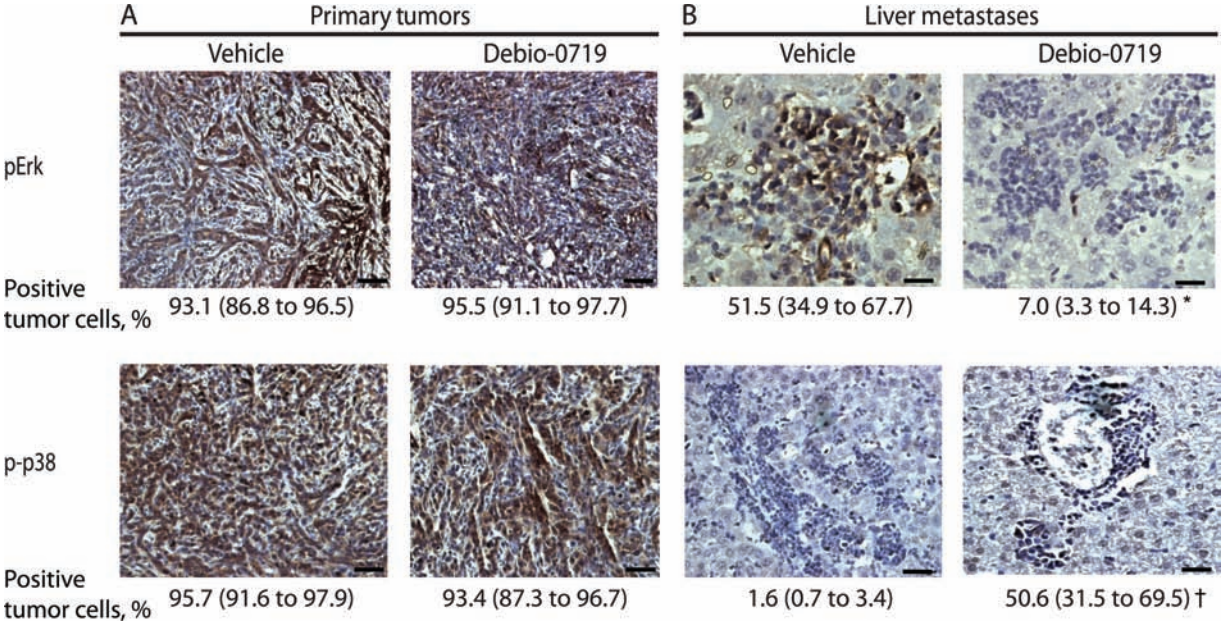

Figure 5. Effect of Debio-0719 on p38 and Erk activation in the 4T1 spontaneous metastasis model. Tissue sections from the **A**) primary tumors and **B**) metastases in the liver from mice injected with 4T1 cells and treated with either vehicle control or Debio-0719 (15 mg/kg administered subcutaneously twice daily) underwent differential immunohistochemical staining for phospho-Erk (pErk) and phospho-p38 (p-p38). Representative images are shown. The mean percentage of cells that stained positive for each antibody are given below each image (n = 5). The corresponding 95% confidence intervals (given in parentheses after the percentage of positive cells below each image) are also reported. **P* =.007 and †P =.002 as calculated by a two-sided *t* test indicate a statistically significant difference in protein expression compared with the vehicle control. Scale bar = 220 μm.

to 15.6%, *P* = .005) (Figure 4, B). Similar trends were observed in 4T1 lung metastases (data not shown). No detectable cleaved caspase 3 was observed at any site (data not shown). Thus, LPA1 pathway interruption inhibited tumor proliferation in a site-specific manner, suggesting that metastatic dormancy was induced.

Metastatic dormancy is widespread in breast, prostate, and other cancers, although the molecular basis is not completely known. Dormancy has been proposed to result from the reciprocal downregulation of the proliferative Erk Map kinase pathway and upregulation of the p38 stress Map kinase pathway (53,54). The percentage of pErk- and phospho-p38-positive tumor cells in primary tumors from vehicle- and Debio-0719-treated mice were comparable (*P* = .55 for both pErk and phospho-p38) (Figure 5, A). In contrast, pErk was consistently downregulated in Debio-0719-treated liver metastases (Figure 5, B), decreasing 86.4%, from 51.5% positivity in the vehicle group to 7.0% in the Debio-0719 group (mean difference = 44.5% of cells positive, 95% CI = 35.6% to 53.4%, *P* = .007). Phospho-p38 positivity showed the opposite pattern in liver metastases, increasing from 1.6% of tumor cells in the vehicle group to 50.6% of Debio-0719-treated tumor cells (mean difference = 49.0% of cells positive, 95% CI = 38.5% to 59.9%, *P* = .002). Similar trends were observed in 4T1 lung metastases (data not shown). The data support the hypothesis that LPA1 inhibition induced metastatic dormancy.

Debio-0719 in a MDA-MB-231T Pulmonary Metastasis Model

To confirm the metastasis suppressor function of Debio-0719, the low Nm23-H1–expressing, hormone receptor–negative MDA-MB-231T human breast carcinoma cell line (50) was injected either in the mammary fat pad to produce primary tumors or in the tail vein to produce experimental lung metastases; mice were randomized to vehicle or Debio-0719 beginning on day 2 postinjection. Primary tumor size 28 days postinjection was not statistically significantly decreased by Debio-0719 (*P* = .98) (Figure 6, A). Within the 42-day time frame of the experimental metastasis assay, 13 (100.0%) of 13 vehicle-treated mice succumbed to breathing difficulties vs 1 (7.7%) of 13 mice receiving continuous Debio-0719 (Figure 6, B, green vs red). Representative lungs from the vehicle and continuous Debio-0719 treatment groups, shown on Figure 6, C, indicate drug-induced metastasis suppression. The median number of surface lung metastases per mouse was 166 in the vehicle group and decreased 77.1% to 38 with continuous Debio-0719 treatment (median difference = 128 metastases per lung, 95% CI = 83 to 170, *P* < .001) (Figure 6, D). A median of seven large metastases (>5 mm in the largest dimension) was present in the vehicle group (Figure 6, E) and decreased 100.0% to a median of 0 in the Debio-0719 group (median difference = 7 metastases per lung, 95% CI = 3 to 8, *P* < .001), indicating suppression of both metastasis number and size.

To determine if continuous Debio-0719 was required for metastasis suppression, a third treatment group was treated with Debio-0719 for 35 days, at which time 14 (100.0%) of 14 mice were alive; thereafter, mice were switched to vehicle. Survival progressively decreased because mice with labored breathing were killed, and pulmonary metastases were evident at necropsy, indicating that suppression of metastasis was reversible (*P* < .05 for all three groups) (Figure 6, B).

The Ki67 proliferative status of MDA-MB-231T experimental lung metastases also suggested induction of dormancy by Debio-0719, which was reversed when treatment was stopped (Supplementary Figure 5, available online). For MDA-MB-231T lung metastases, which harbor Ras and B-Raf mutations (55), constitutively activated pErk was observed under all conditions. However, Debio-0719

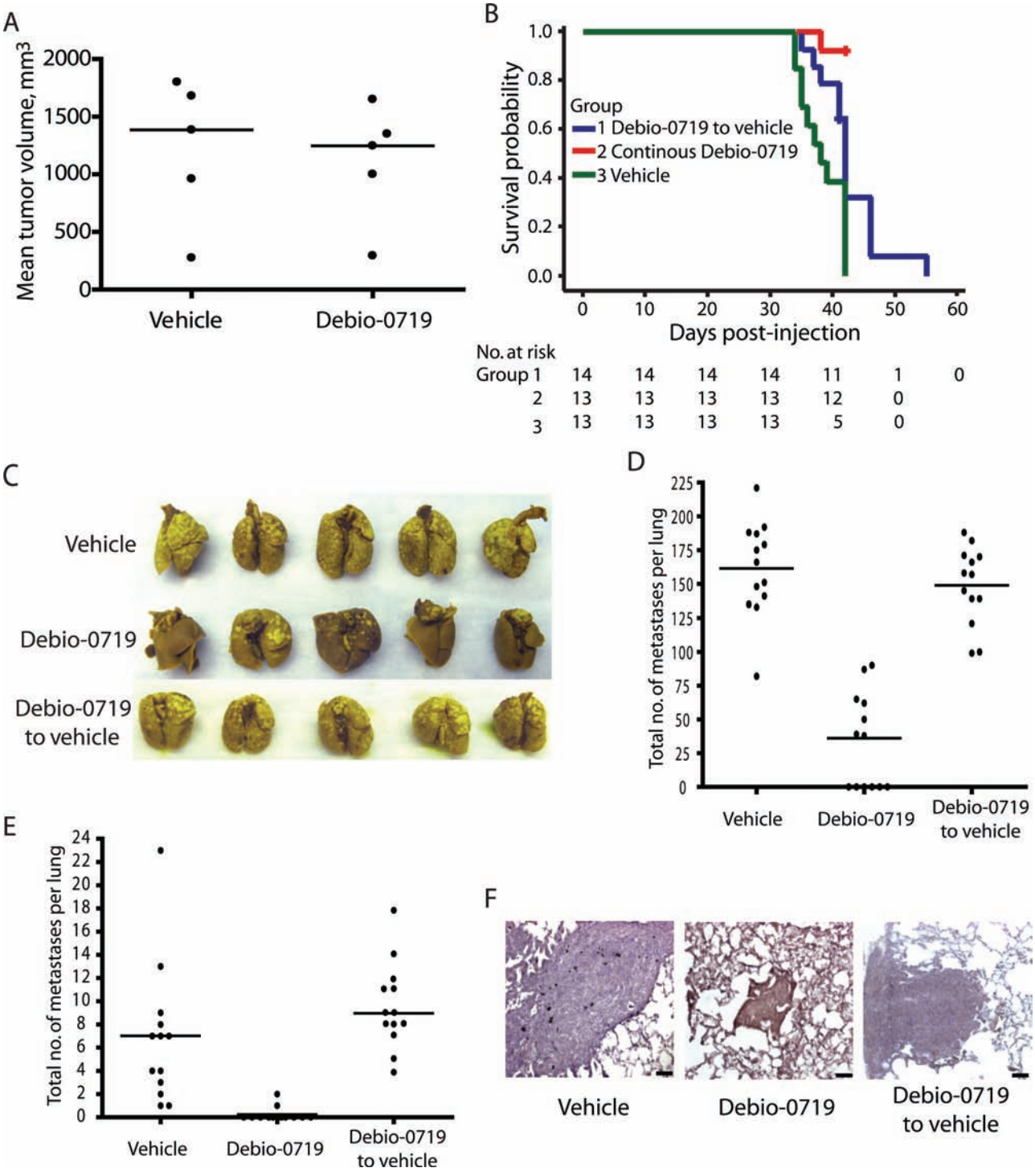

Figure 6. Effect of Debio-0719 on primary tumor size and experimental pulmonary metastasis in the MDA-MB-231T mouse model. **A**) MDA-MB-231T cells were injected into the mammary fat pads of athymic NRC nu/nu mice. The day following implantation, mice were randomized into two groups (n = 5) and administered either vehicle control or 15 mg/kg Debio-0719 given subcutaneously twice daily. Mice were killed on day 32. The median volume of the primary tumors on day 32 is depicted by the **bars**. **B–D**) MDA-MB-231T cells were injected into the tail veins of athymic NRC nu/nu mice on day 0. On the following day, the mice were randomized into groups (n = 13 or 14) and treated with vehicle, 15 mg/kg Debio-0719 subcutaneously twice daily, or 15 mg/kg Debio-0719 subcutaneously twice daily for 35 days postinjection and then administered vehicle thereafter. Mice were killed when breathing distress was observed. **B**) Kaplan–Meier survival curves are shown, and the number of mice at risk is given in the table below. Censored data is indicated by a **+**. **C**) Representative pictures of the lungs harvested from the mice in each treatment group are shown. The metastases are indicated by the lighter nodules that are apparent on the surface of the lungs. **D**) The dot plot shows the total number of metastatic nodules on the surface of the lungs from mice in each group. Any nodule larger than 5 mm in size was classified separately as a large metastasis, and these data are shown separately in (**E**). The median of each group is indicated by the **bar**. **F**) Lung tissues from mice shown in panels (**B–D**) underwent immunohistochemical staining for phospho-p38. Scale bar = 220 μm.

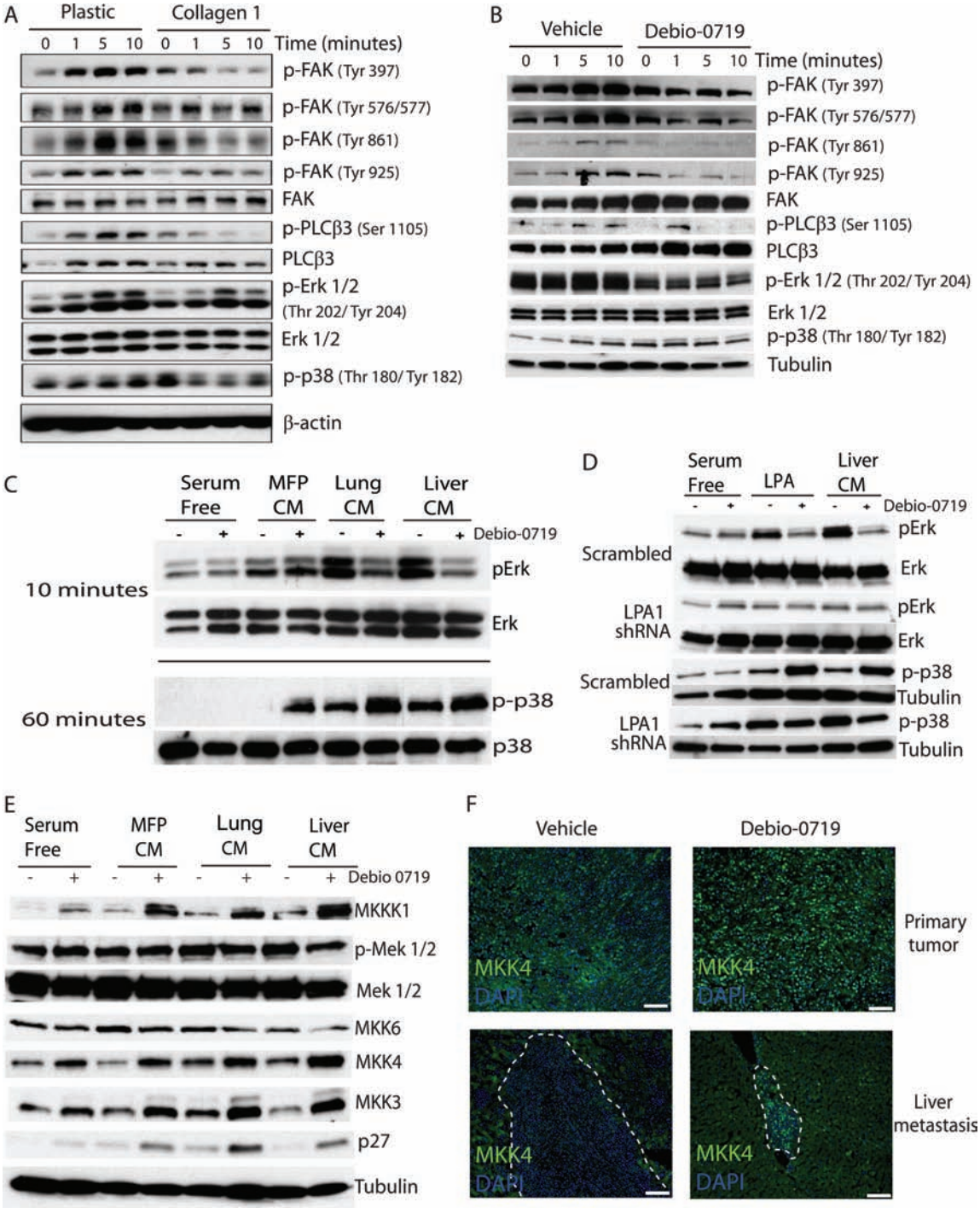

Figure 7. Effect of lysophosphatidic acid receptor 1 (LPA1) inhibition on p38 activation in vitro. **A**) 4T1 cells were plated on plastic or type I collagen-coated cell culture plates, were serum-starved overnight, and then stimulated with 5 μM lysophosphatidic acid (LPA) for 0, 1, 5, or 10 minutes. Cell lysates were prepared, and western blotting for total and phosphorylated proteins, including focal adhesion kinase (FAK), phospholipase Cβ (PLCβ), Erk1/2, p38, and β actin (loading control), was done. **B**) 4T1 cells were plated on type I collagen-coated plates, serum-starved overnight, and treated with vehicle control or 60 nM Debio-0719. Cells were then stimulated with LPA for 0, 1, 5, or 10 minutes. Cell lysates were prepared, and western blotting for total and phosphorylated proteins, including FAK, PLCβ, Erk1/2, p38, and tubulin (loading control), was done. **C**) 4T1 cells were cultured on type I collagen-coated culture plates in the presence of 60 nM Debio-0719 and then serum-starved and stimulated with 20% (v/v) conditioned medium (CM) from liver, lungs, or mammary fat pads (MFP) for 10 or 60 minutes. Phosphorylated and total Erk and p38 protein levels were determined by western blot. **D**) 4T1 cells expressing LPA1 short hairpinned (shRNA) or a scrambled control shRNA were cultured on type I collagen-coated plates in the presence of 60 nM Debio-0719 or vehicle control and then serum-starved and stimulated with 20% (v/v) conditioned medium (CM) from liver, serum-free medium, or LPA only for 1 hour. Phosphorylated and total Erk and p38 protein levels were determined by western blot. Tubulin served as the loading control. **E**) 4T1 cells were cultured as described in panel (**C**), but lysates were prepared after 10 minutes of stimulation with CM, serum-free medium, and probed for total and phosphorylated MAP kinases. The images shown for (**A**–**E**) are representative of three independent experiments. **F**) Immunofluorescent images of MKK4 expression (**green**) in primary tumors or liver metastases (**white dashed line**) from either vehicle- or Debio-0719-treated primary tumor and liver tissues from mice used in the experiments described in Figure 2, B–E. Nuclei were stained with 4′,6-diamidino-2-phenylindole (DAPI, **blue**). Scale bar = 220 μm.

elevated phospho-p38 in pulmonary metastases (Figure 6, F). In conclusion, the Debio-0719 compound suppressed metastasis in two model systems, with p38 activation a consistent hallmark.

Contributors to Increased p38 Signaling in Metastatic Dormancy

It is clear that metastatic dormancy in our model systems results from signaling that is distinct between the primary tumor and the distant metastases, as well as between normal conditions and LPA1 inhibition. LPA1 interacts with G-protein-coupled receptors to signal via multiple downstream pathways conferring tumor motility and invasion (56–62) as well as other phenotypes. When 4T1 cells were cultured with serum on plastic, treatment with LPA activated focal adhesion kinase and phospholipase Cβ (PLCβ) signaling, typical of motility and invasion, as well as Erk (Thr 202/Tyr 204); no effect on p38 activation was observed (Figure 7, A). Histologic analysis indicated that 4T1 cells, in metastasizing to the liver, migrated from the portal venules of the liver past the basement membrane to the perivascular space, which is enriched for type I collagen (Supplementary Figure 6, A, available online); similar observations were made in the lung. In agreement with this observation, 4T1 cells adhered preferentially to type I collagen (Supplementary Figure 6, B, available online). When 4T1 cells were cultured with serum on type I collagen, the resulting signaling pattern recapitulated those observed in vivo to show LPA activation of Erk and diminution of phospho-p38 (Figure 7, A), which was inhibited by Debio-0719 treatment (Figure 7, B).

In examining the primary vs metastatic sites, we hypothesized that soluble factors present in the mammary fat pad vs liver and lung microenvironments may contribute to differential signaling patterns. Conditioned medium was prepared from freshly isolated primary cultures of dissected mouse mammary fat pads, lung fibroblasts, and parenchymal and nonparenchymal liver cells. Using cytokine arrays, 29 cytokines were overexpressed in conditioned media prepared from the lung and liver compared with conditioned medium from the mammary fat pad (Supplementary Figure 7, available online). The role of these conditioned media in metastatic dormancy signaling was investigated by culturing 4T1 cells on type I collagen, in the presence of various conditioned media (Figure 7, C). Erk was activated in 4T1 cells by lung and nonparenchymal liver–conditioned media to a greater degree than mammary fat pad–conditioned medium; activation was inhibited by Debio-0719 to recapitulate the observed in vivo expression trends. For p38, activation was stimulated by Debio-0719 over a longer time course, to a greater degree in the presence of liver and lung–conditioned media than with mammary fat pad–conditioned medium. These expression patterns were not observed when tumor cells were plated on plastic or type IV collagen (data not shown). Similar trends were observed using scrambled vs LPA1 shRNA knockdown 4T1 cells (Figure 7, D). Thus, in vitro culture of 4T1 cells on type I collagen in the presence of organ–conditioned medium modeled aspects of the in vivo metastasis data.

We further hypothesized that inhibition of LPA1 signaling specifically promoted p38 activation, regardless of the initiating stimulus. The p38 stress Map kinase is activated by Map2Ks (MKK3, MKK6, MKK4, and MKK7 can activate p38 or Jun kinase) and Map3Ks (MKKs, TAK, and others) (63). When cultured on type I collagen, 4T1 cells expressed increased levels of total MKKK1, MKK3, and MKK4 in response to Debio-0719, regardless of the presence or type of conditioned medium (Figure 7, E). In agreement with these data, MKK4 expression was upregulated in liver metastases of Debio-0719 treated mice (Figure 7, F). Of the phospho-p38 MAP2Ks, MKK3 showed the highest levels of induction of total protein in response to LPA1 inhibition, and it signals directly to p38. One of the known targets of p38 is the cell cycle inhibitor p27 (64,65). In agreement with the p38 activation data, Debio-0719 enhanced p27 expression in vitro and in vivo (Figure 7, E and Supplementary Figure 8, available online). Collectively, the data suggest that the hyperactivation of p38 seen in metastatic dormancy may result from an abundance of stimulants in the metastatic microenvironment coupled with overexpression of pathway constituents in response to LPA1 inhibition.

Discussion

On the basis of the inverse expression and functional interaction of Nm23-H1 and LPA1 (26,27), we hypothesized that a LPA1 inhibitor could function as a metastasis suppressor. Debio-0719 statistically significantly inhibited the metastasis of 4T1 murine mammary cells to the lungs and liver in four different spontaneous metastasis experiments. In the MDA-MB-231T human breast carcinoma model, Debio-0719 statistically significantly inhibited the formation of pulmonary metastases. Mouse survival was dependent on continuous Debio-0719 administration. These data agree with previous reports using various LPA1 pathway inhibitors assessing aspects of metastasis (39,66). LPA1 knockdown also statistically significantly prevented metastasis formation in the 4T1 model system, indicating that the effect of Debio-0719 is largely LPA1-specific and that the effects resulting from pharmacological inhibition of LPA1 can be recapitulated by knocking down LPA1.

LPA1 inhibition did not statistically significantly reduce primary tumor size in any experiment we performed, suggesting that the LPA1 pathway has no major role in tumor initiation and maintenance at the primary site in our model systems. Thus, LPA1 inhibition has the properties of a metastasis suppressor (2,5,67). The Debio-0719 compound was nontoxic in our experiments, indicating that LPA1 can be targeted with a good safety margin; currently, various compounds directed at this pathway are under development (68). Previous reports have similarly demonstrated distinct responses in primary and metastatic sites to changes in tumor cell gene expression or drugs (69–71). Because virtually all cancer therapeutics currently in use were validated by short-term inhibition of subcutaneous tumor growth as a preclinical endpoint, the LPA1 inhibitor, Debio-0719, would have been missed by traditional validation strategies.

Our data also indicate that LPA1 pathway inhibition induced aspects of metastatic dormancy. Dormancy, the long-term persistence of subclinical solitary or micrometastatic tumor cells, is poorly understood, and it has been characterized as reflecting a balance of proliferation and apoptosis, cell cycle quiescence, immunological surveillance, or other mechanisms (72–79). In previous studies, when tested, dormant tumor cells were insensitive to traditional chemotherapeutics (80). A translational goal in breast cancer is to induce or sustain a chronic dormant phenotype in tumor cells. In our

model systems, LPA1 inhibition reduced the percentage of tumor cells transiting the cell cycle only in the metastatic sites—not in the primary tumor. Opposing activation of the p38 stress kinase and inactivation of the Erk Map kinase have been reported as a potential hallmark of dormancy (53,54,81). This pattern was confirmed in the metastatic lesions (but not primary tumors) of the two model systems, with the exception of Erk activation in MDA-MB-231T cells, which was constitutively activated by Ras/Raf mutations.

Activation of p38 was a consistent indicator of dormancy in the 4T1 and MDA-MB-231T models studied. Selective activation of p38 in metastatic lesions may result from the multitude of cytokines present in the liver and lungs, many of which are known to induce p38 stress responses (82–97). We hypothesize that the LPA1 pathway serves as a gatekeeper for many of these cytokines to activate p38: Inhibition of LPA1, by Debio-0719 or shRNA targeting LPA1, resulted in the upregulation of components of the p38 stress kinase pathway at the protein level, including MKK3, MKK4, and MKKK1. Thus, signaling that activates p38 from a multitude of cytokines present in the metastatic microenvironments could be amplified by overexpression of pathway constituents. It is noteworthy that MKK4 is a validated metastasis suppressor gene (98); thus, one mode of action of a metastasis-suppressive compound may be the elevation of other suppressor proteins. To our knowledge, Debio-0719 is one of the first compounds to induce metastatic dormancy in triple negative breast cancer cells. As a monotherapy, this type of inhibitor would be likely to have minimal activity in the advanced metastatic setting of phase I trials, but it would be expected to be effective in the adjuvant setting, which is similar to the design of the preclinical experiments. Adjuvant setting trials are large and costly, and therefore they are unsuitable for validating potential metastasis-suppressive drugs such as Debio-0719. Rather, we propose that initial clinical testing use pre- and post-treatment tumor biopsies to determine the effect of drug on Ki67, pErk, and phospho-p38 levels; phase II efficacy trials could enroll high-risk patients to determine relapse-free survival.

Our study is not without limitations. Our experiments did not determine the duration of the dormancy response to LPA1 inhibition. Also, Debio-0719 should be tested in other model systems. Other LPA1-linked and -independent signaling pathways also likely mediate metastatic dormancy, and further studies are necessary to identify these pathways.

In summary, a new drug development paradigm is presented to induce tumor dormancy in metastatic sites. Inhibition of signaling by the ubiquitous serum phospholipid LPA through the LPA1 receptor resulted in tumor withdrawal from the cell cycle in metastatic niches and a statistically significant prevention of metastasis formation. With such inhibitors in hand, the interaction of dormancy pathways and standard of care therapeutics, radiation therapy, patient stress, and other important factors can be determined to develop a deeper picture of potential preventative and therapeutic scenarios.

References

1. Yoshida B, Sokoloff M, Welch D, Rinker-Schaeffer C. Metastasis-suppressor genes: a review and perspective on an emerging field. *J Natl Cancer Inst*. 2000;92(21):1717–1730.
2. Steeg P. Metastasis suppressors alter the signal transduction of cancer cells. *Nat Cancer Rev*. 2003;3(1):55–63.
3. Rinker-Schaeffer CW, O'Keefe JP, Welch DR, Theodorescu D. Metastasis suppressor proteins: discovery, molecular mechanisms, and clinical application. *Clin Cancer Res*. 2006;12(13):3882–3889.
4. Kauffman E, Robinson V, Stadler W, Sokoloff M, Rinker-Schaeffer C. Metastasis suppression: the evolving role of metastasis suppressor genes for regulating cancer cell growth at the secondary site. *J Urol*. 2003;169(3):1122–1133.
5. Smith S, Theodorescu D. Learning therapeutic lessons from metastasis suppressor proteins. *Nat Rev Cancer*. 2009;9(4):253–264.
6. Stafford LJ, Vaidya KS, Welch DR. Metastasis suppressors genes in cancer. *Int J Biochem Cell Biol*. 2008;40(5):874–891.
7. Steeg PS, Bevilacqua G, Kopper L, et al. Evidence for a novel gene associated with low tumor metastatic potential. *J Natl Cancer Inst*. 1988;80(3):200–204.
8. Rosengard AM, Krutzsch HC, Shearn A, et al. Reduced Nm23/Awd protein in tumour metastasis and aberrant Drosophila development. *Nature*. 1989;342(6246):177–180.
9. Leone A, Flatow U, King CR, et al. Reduced tumor incidence, metastatic potential, and cytokine responsiveness of nm23-transfected melanoma cells. *Cell*. 1991;65(1):25–35.
10. Subramanian C, Cotter M, Robertson E. Epstein-Barr virus nuclear protein EBNA-3C interacts with the human metastatic suppressor Nm23-H1: a molecular link to cancer metastasis. *Nat Med*. 2001;7(3):350–355.
11. Leone A, Flatow U, VanHoutte K, Steeg PS. Transfection of human nm23-H1 into the human MDA-MB-435 breast carcinoma cell line: effects on tumor metastatic potential, colonization and enzymatic activity. *Oncogene*. 1993;8(9):2325–2333.
12. Bhujwalla Z, Aboagye E, Gillies R, Chacko V, Mendola C, Backer J. Nm23-transfected MDA-MB-435 human breast carcinoma cells form tumors with altered phospholipid metabolism and pH: a 31P nuclear magnetic resonance study in vivo and in vitro. *Magn Reson Med*. 1999;41(5):897–903.
13. Russell R, Geisinger K, Mehta R, White W, Shelton B, Kute T. nm23–relationship to the metastatic potential of breast carcinoma cell lines, primary human xenografts, and lymph node negative breast carcinoma patients. *Cancer*. 1997;79(6):1158–1165.
14. Fukuda M, Ishii A, Yasutomo Y, et al. Decreased expression of nucleoside diphosphate kinase alpha isoform, an nm23-H2 gene homolog, is associated with metastatic potential of rat mammary-adenocarcinoma cells. *Int J Cancer*. 1996;65(4):531–537.
15. Baba H, Urano T, Okada K, et al. Two isotypes of murine nm23/nucleoside diphosphate kinase, nm23-M1 and nm23-M2, are involved in metastatic suppression of a murine melanoma line. *Cancer Res*. 1995;55(9):1977–1981.
16. Miele ME, Rosa ADL, Lee JH, et al. Suppression of human melanoma metastasis following introduction of chromosome 6 is independent of NME1 (Nm23). *Clin Exp Metastasis*. 1997;15(3):259–265.
17. Parhar RS, Shi Y, Zou M, Farid NR, Ernst P, Al-Sedairy S. Effects of cytokine-mediated modulation of nm23 expression on the invasion and metastatic behavior of B16F10 melanoma cells. *Int J Cancer*. 1995;60(2):204–210.
18. Tagashira H, Hamazaki K, Tanaka N, Gao C, Namba M. Reduced metastatic potential and c-myc overexpression of colon adenocarcinoma cells (Colon 26 line) transfected with nm23-R2/rat nucleoside diphosphate kinase alpha isoform. *Int J Mol Med*. 1998;2(1):65–68.
19. Miyazaki H, Fukuda M, Ishijima Y, et al. Overexpression of nm23-H2/NDP kinase B in a human oral squamous cell carcinoma cell line results in reduced metastasis, differentiated phenotype in the metastatic site, and growth factor-independent proliferative activity in culture. *Clin Cancer Res*. 1999;5(12):4301–4307.
20. Suzuki E, Ota T, Tsukuda K, et al. nm23-H1 reduces in vitro cell migration and the liver metastatic potential of colon cancer cells by regulating myosin light chain phosphorylation. *Int J Cancer*. 2004;108(2):207–211.
21. Che G, Chen J, Liu L, et al. Transfection of nm23-H1 increased expression of beta-Catenin, E-Cadherin and TIMP-1 and decreased the expression of MMP-2, CD44v6 and VEGF and inhibited the metastatic potential of human non-small cell lung cancer cell line L9981. *Neoplasma*. 2006;53(6):530–537.
22. D'Angelo A, Garzia L, André A, et al. Prune cAMP phosphodiesterase binds nm23-H1 and promotes cancer metastasis. *Cancer Cell*. 2004;5(2):137–149.

23. Boissan M, Wendum D, Arnaud-Dabernat S, et al. Increased lung metastasis in transgenic NM23-Null/SV40 mice with hepatocellular carcinoma. *J Natl Cancer Inst*. 2005;97(11):836–845.
24. Titus B, Frierson HF Jr, Conaway M, et al. Endothelin axis is a target of the lung metastasis suppressor gene RhoGDI2. *Cancer Res*. 2005;65(16):7320–7327.
25. Sur S, Pagliarini T, Bunz F, et al. A panel of isogenic human cancer cells suggests a therapeutic approach for cancers with inactivated p53. *Proc Natl Acad Sci U S A*. 2009;106(9):3064–3969.
26. Horak CE, Lee JH, Elkahloun AG, et al. Nm23-H1 suppresses tumor cell motility by down-regulating the lysophosphatidic acid receptor EDG2. *Cancer Res*. 2007;67(15):7238–7246.
27. Horak CE, Mendoza A, Vega-Valle E, et al. Nm23-H1 suppresses metastasis by inhibiting expression of the lysophosphatidic acid receptor EDG2. *Cancer Res*. 2007;67(24):11751–11759.
28. Murph MM, Nguyen GH, Radhakrishna H, Mills GB. Sharpening the edges of understanding the structure/function of the LPA1 receptor: expression in cancer and mechanisms of regulation. *Biochim Biophys Acta*. 2008;1781(9):547–557.
29. Contos JJ, Ishii I, Chun J. Lysophosphatidic acid receptors. *Mol Pharmacol*. 2000;58(6):1188–1196.
30. Takuwa Y, Takuwa N, Sugimoto N. The Edg family G protein-coupled receptors for lysophospholipids: their signaling properties and biological activities. *J Biochem*. 2002;131(6):767–771.
31. Luquain C, Sciorra VA, Morris AJ. Lysophosphatidic acid signaling: how a small lipid does big things. *Trends Biochem Sci*. 2003;28(7):377–383.
32. Moolenaar WH, van Meeteren LA, Giepmans BN. The ins and outs of lysophosphatidic acid signaling. *Bioessays*. 2004;26(8):870–881.
33. Mills G, Moolenaar W. The emerging role of lysophosphatidic acid in cancer. *Nat Rev Cancer*. 2003;3(8):582–591.
34. Anliker B, Chun J. Lysophospholipid G protein-coupled receptors. *J Biol Chem*. 2004;279(20):20555–20558.
35. Aoki J, Taira A, Takanezawa Y, et al. Serum lysophosphatidic acid is produced through diverse phospholipase pathways. *J Biol Chem*. 2002;277(4):48737–48744.
36. Liu S, Umezu-Goto M, Murph M, et al. Expression of autotaxin and lysophosphatidic acid receptors increases mammary tumorigenesis, invasion, and metastases. *Cancer Cell*. 2009;15(6):539–550.
37. Chen M, Towers LN, O'Connor KL. LPA2 (EDG4) mediates Rho-dependent chemotaxis with lower efficacy than LPA1 (EDG2) in breast carcinoma cells. *Am J Physiol, Cell Physiol*. 2007;292(5): C1927–C1933.
38. Hama K, Aoki J, Fukaya M, et al. Lysophosphatidic acid and autotaxin stimulate cell motility of neoplastic and non-neoplastic cells through LPA1. *J Biol Chem*. 2004;279(1):17634–17639.
39. Boucharaba A, Serre CM, Guglielmi J, Bordet JC, Clézardin P, Peyruchaud O. The type 1 lysophosphatidic acid receptor is a target for therapy in bone metastases. *Proc Natl Acad Sci USA*. 2006;103(25):9643–9648.
40. Shida D, Kitayama J, Yamaguchi H, et al. Lysophosphatidic acid (LPA) enhances the metastatic potential of human colon carcinoma DLD1 cells through LPA1. *Cancer Res*. 2003;63(7):1706–1711.
41. Komachi M, Tomura H, Malchinkhuu E, et al. LPA1 receptors mediate stimulation, whereas LPA2 receptors mediate inhibition, of migration of pancreatic cancer cells in response to lysophosphatidic acid and malignant ascites. *Carcinogenesis*. 2009;30(3):457–465.
42. Waters C, Saatian B, Moughal N, et al. Integrin signalling regulates the nuclear localization and function of the lysophosphatidic acid receptor-1 (LPA1) in mammalian cells. *Biochem J*. 2006;398(1):55–62.
43. Yu S, Murph M, Lu Y, et al. Lysophosphatidic acid receptors determine tumorigenicity and agressiveness of ovarian cancer cells. *J Natl Cancer Inst*. 2008;20(22):1630–1642.
44. Zhang H, Xu X, Gajewiak J, et al. Dual activity lysophosphatidic acid receptor pan-antagonist/autotaxin inhibitor reduces breast cancer cell migration in vitro and causes tumor regression in vivo. *Cancer Res*. 2009;69(13):5441–5449.
45. Peyruchaud O. Novel implications for lysophospholipids, lysophosphatidic acid and sphingosine 1-phosphate, as drug targets in cancer. *Anticancer Agents Med Chem*. 2009;9(4):381–391.
46. Kano K, Arima N, Ohgami M, Aoki J. LPA and its analogs-attractive tools for elucidation of LPA biology and drug development. *Curr Med Chem*. 2008;15(21):2122–2131.
47. Ohta H, Sato K, Murata N, et al. Ki16425, a subtype-selective antagonist for EDG-family lysophosphatidic acid receptors. *Mol Pharmacol*. 2003;64(4):994–1005.
48. Prestwich G, Gajewiak J, Zhang H, Xu X, Yang G, Serban M. Phosphatase-resistant analogues of lysophosphatidic acid: agonists promote healing, antagonists and autotaxin inhibitors treat cancer. *Biochim Biophys Acta*. 2008;1781(9):588–594.
49. Mukai M, Imamura F, Ayaki M, et al. Inhibition of tumor invasion and metastasis by a novel lysophosphatidic acid (cyclic LPA). *Int J Cancer*. 1999;81(6):918–922.
50. Palmieri D, Halverson D, Ouatas T, et al. Medroxyprogesterone acetate elevation of Nm23-H1 metastasis suppressor expression in hormone receptor-negative breast cancer. *J Natl Cancer Inst*. 2005;97(9):632–642.
51. Fitzgerald D, Palmieri D, Hua E, et al. Reactive glia are recruited by highly proliferative brain metastases of breast cancer and promote tumor cell colonization. *Clin Exp Metastasis*. 2008;25(7):799–810.
52. Tao K, Fang M, Alroy J, Sahagian GG. Imagable 4T1 model for the study of late stage breast cancer. *BMC Cancer*. 2008;8:228.
53. Aguirre-Ghiso J, Estrada Y, Liu D, Ossowski L. ERK(MAPK) activity as a determinant of tumor growth and dormancy; regulation by p38(SAPK). *Cancer Res*. 2003;63(7):1684–1695.
54. Aguirre-Ghiso JA, Ossowski L, Rosenbaum SK. Green fluorescent protein tagging of extracellular signal-regulated kinase and p38 pathways reveals novel dynamics of pathway activation during primary and metastatic growth. *Cancer Res*. 2004;64(20):7336–7345.
55. Hollestelle A, Elstrodt F, Nagel JH, Kallemeijn WW, Schutte M. Phosphatidylinositol-3-OH kinase or RAS pathway mutations in human breast cancer cell lines. *Mol Cancer Res*. 2007;5(2):195–201.
56. Li T, Alemayehu M, Aziziyeh A, et al. Beta-arrestin/Ral signaling regulates lysophosphatidic acid-mediated migration and invasion of human breast tumor cells. *Mol Cancer Res*. 2009;7(7):1064–1077.
57. Park S, Schinkmann K, Avraham S. RAFTK/Pyk2 mediates LPA-induced PC12 cell migration. *Cell Signal*. 2006;18(7):1063–1071.
58. Sawada K, Morishige K, Tahara M, et al. Lysophosphatidic acid induces focal adhesion assembly through Rho/Rho-associated kinase pathway in human ovarian cancer cells. *Gynecol Oncol*. 2002;87(3):252–259.
59. Bian D, Mahanivong C, Yu J, et al. The G12/13-RhoA signaling pathway contributes to efficient lysophosphatidic acid-stimulated cell migration. *Oncogene*. 2006;25(15):2234–2244.
60. Bian D, Su S, Mahanivong C, et al. Lysophosphatidic acid stimulates ovarian cancer cell migration via a Ras-MEK kinase 1 pathway. *Cancer Res*. 2004;64(12):4209–4217.
61. Jung I, Lee J, Lee K, et al. Activation of p21-activated kinase 1 is required for lysophosphatidic acid-induced focal adhesion kinase phosphorylation and cell motility in human melanoma A2058 cells. *Eur J Biochem*. 2004;271(8):1557–1565.
62. Malchinkhuu E, Sato K, Horiuchi Y, et al. Role of p38 mitogen-activated kinase and c-Jun terminal kinase in migration response to lysophosphatidic acid and sphingosine-1-phosphate in glioma cells. *Oncogene*. 2005;24(44):6676–6688.
63. Keshet Y, Seger R. *The MAP Kinase Signaling Cascades: A System of Hundreds of Components Regulates a Diverse Array of Physiological Functions*. 2nd ed. New York, NY: Springer; 2010.
64. Adler H, Steinbrink K. MAP kinase p38 and its relation to T cell anergy and suppressor function of regulatory T cells. *Cell Cycle*. 2008;7(2):169–170.
65. Pillai M, Sapna S, Shivakumar K. p38 MAPK regulates G1-S transition in hypoxic cardiac fibroblasts. *Int J Biochem Cell Biol*. 2011;43(6):919–927.
66. Inokuchi M, Uetake H, Shirota Y, Yamada H, Tajima M, Sugihara K. Gene expression of 5-fluorouracil metabolic enzymes in primary colorectal cancer and corresponding liver metastasis. *Cancer Chemother Pharmacol*. 2004;53(5):391–396.
67. Taylor J, Hickson J, Lotan T, Yamada DS, Rinker-Schaeffer C. Using metastasis suppressor proteins to dissect interactions among cancer cells and their microenvironment. *Cancer Metastasis Rev*. 2008;27(1):67–73.
68. Swaney J, Chapman C, Correa L, et al. A novel, orally active LPA(1) receptor antagonist inhibits lung fibrosis in the mouse bleomycin model. *Br J Pharmacol*. 2010;160(7):1699–1713.

69. Steeg P, Theodorescu D. Metastasis: a therapeutic target for cancer. *Nat Clin Pract Oncol*. 2008;5(4):206–219.
70. Steeg PS. Tumor metastasis: mechanistic insights and clinical challenges. *Nat Med*. 2006;12(8):895–904.
71. Stoecklein N, Klein C. Genetic disparity between primary tumours, disseminated tumour cells, and manifest metastasis. *Int J Cancer*. 2010;126(3):589–598.
72. Goss P, Chambers A. Does tumour dormancy offer a therapeutic target? *Nat Rev Cancer*. 2010;10(12):871–877.
73. Aguirre-Ghiso J. Models, mechanisms and clinical evidence for cancer dormancy. *Nat Rev Cancer*. 2007;7(11):834–846.
74. Noltenius C, Noltenius H. Dormant tumor cells in liver and brain. An autopsy study on metastasizing tumors. *Pathol Res Pract*. 1985;179(4-5):504–511.
75. Goodison S, Kawai K, Hihara J, et al. Prolonged dormancy and site-specific growth potential of cancer cells spontaneously disseminated from nonmetastatic breast tumors as revealed by labeling with green fluorescent protein. *Clin Cancer Res*. 2003;9(10 Pt 1):3808–3814.
76. Cao Y, O'Reilly MS, Marshall B, Flynn E, Ji RW, Folkman J. Expression of angiostatin cDNA in a murine fibrosarcoma suppresses primary tumor growth and produces long-term dormancy of metastases. *J Clin Invest*. 1998;101(5):1055–1063.
77. McAllister S, Gifford A, Greiner A, et al. Systemic endocrine instigation of indolent tumor growth requires osteopontin. *Cell*. 2008;133(6):994–1005.
78. Willis L, Alarcón T, Elia G, et al. Breast cancer dormancy can be maintained by small numbers of micrometastases. *Cancer Res*. 2010;70(11):4310–4317.
79. Uhr J, Pantel K. Controversies in clinical cancer dormancy. *Proc Natl Acad Sci USA*. 2011;108(30):12396–12400.
80. Naumov G, Townson J, MacDonald I, et al. Ineffectiveness of doxorubicin treatment on solitary dormant mammary carcinoma cells or late-developing metastases. *Breast Cancer Res Treat*. 2003;82(3):199–206.
81. Shin J-S, Woo S, Lee H-C, et al. Low doses of ionizing radiation suppress doxorubicin-induced senescence-like phenotypes by activation of ERK1/2 and suppression of p38 kinase in MCF7 human breast cancer cells. *Int J Oncol*. 2010;36(6):1445–1452.
82. Bertelsen M, Sanfridson A. TAB1 modulates IL-1alpha mediated cytokine secretion but is dispensable for TAK1 activation. *Cell Signal*. 2007;19(3):646–657.
83. Ogata S, Kubota Y, Yamashiro T, et al. Signaling pathways regulating IL-1alpha-induced COX-2 expression. *J Dent Res*. 2007;86(2):186–191.
84. Santos L, Fan H, Hall P, et al. Macrophage migration inhibitory factor regulates neutrophil chemotactic responses in inflammatory arthritis in mice. *Arthritis Rheum*. 2011;63(4):960–970.
85. Kumar V, Behera R, Lohite K, Karnik S, Kundu G. p38 kinase is crucial for osteopontin-induced furin expression that supports cervical cancer progression. *Cancer Res*. 2010;70(24):10381–10391.
86. Thömmes K, Hoppe J, Vetter H, Sachinidis A. The synergistic effect of PDGF-AA and IGF-1 on VSMC proliferation might be explained by the differential activation of their intracellular signaling pathways. *Exp Cell Res*. 1996;226(1):59–66.
87. Odemis V, Boosmann K, Heinen A, Küry P, Engele J. CXCR7 is an active component of SDF-1 signalling in astrocytes and Schwann cells. *J Cell Sci*. 2010;123(Pt 7):1081–1088.
88. Bigelow R, Williams B, Carroll J, Daves L, Cardelli J. TIMP-1 overexpression promotes tumorigenesis of MDA-MB-231 breast cancer cells and alters expression of a subset of cancer promoting genes in vivo distinct from those observed in vitro. *Breast Cancer Res Treat*. 2009;117(1):31–44.
89. Li Y, Li Y, Qian Z, Ryu B, Kim S. Suppression of vacular endothelial growth factor (VEGF) induced angiogenic responses by fucodiphloroethol G. *Process Biochem*. 2011;46(5):1095–1103.
90. Peters I, Tossidou I, Achenbach J, et al. IGF-binding protein-3 modulates TGF-beta/BMP-signaling in glomerular podocytes. *J Am Soc Nephrol*. 2006;17(6):1644–1656.
91. Hua F, Henstock P, Tang B. ERK activation by GM-CSF reduces effectiveness of p38 inhibitor on inhibiting TNFalpha release. *Int Immunopharmacol*. 2010;10(7):730–737.
92. Fan S, Meng Q, Laterra J, Rosen E. Role of Src signal transduction pathways in scatter factor-mediated cellular protection. *J Biol Chem*. 2009;284(12):7561–7577.
93. Kim Y, Min K, Jeong D, Jang J, Kim H, Kim E. Effects of fibroblast growth factor-2 on the expression and regulation of chemokines in human dental pulp cells. *J Endod*. 2010;36(11):1824–1830.
94. Klosowska K, Volin M, Huynh N, Chong K, Halloran M, Woods J. Fractalkine functions as a chemoattractant for osteoarthritis synovial fibroblasts and stimulates phosphorylation of mitogen-activated protein kinases and Akt. *Clin Exp Immunol*. 2009;156(2):312–319.
95. Campbell M, Collery R, McEvoy A, Gardiner T, Stitt A, Brankin B. Involvement of MAPKs in endostatin-mediated regulation of blood-retinal barrier function. *Curr Eye Res*. 2006;31(12):1033–1045.
96. Zhu Y, Sun Y, Xie L, Jin K, Sheibani N, Greenberg D. Hypoxic induction of endoglin via mitogen-activated protein kinases in mouse brain microvascular endothelial cells. *Stroke*. 2003;10(10):2483–2488.
97. Yamochi T, Yamochi T, Aytac U, et al. Regulation of p38 phosphorylation and topoisomerase IIalpha expression in the B-cell lymphoma line Jiyoye by CD26/dipeptidyl peptidase IV is associated with enhanced in vitro and in vivo sensitivity to doxorubicin. *Cancer Res*. 2005;65(5):1973–1983.
98. Griend D, Kocherginsky M, Hickson J, Stadler W, Lin A, Rinker-Schaeffer C. Suppression of metastatic colonization by the context-dependent activation of the c-Jun NH2-terminal kinase kinases JNKK1/MKK4 and MKK7. *Cancer Res*. 2005;65(23):10984–10991.

Funding

Intramural program of the National Cancer Institute and Breast Cancer Research Stamp Fund awarded through competitive peer review by the National Cancer Institute (to PSS); ISCIII (ADE09/90041) and the Burdinola Professorship on Molecular Medicine (to FV-V).

Notes

The funders did not have a role in the design of the study; the collection, analysis, and interpretation of the data; the writing of the article; and the decision to submit the article for publication. The authors thank Dr Gary Sahagian, Tufts University, for luciferase-labeled 4T1 cells. M. Barbier and M. Murone are employees of Debiopharm S.A.

Affiliations of authors: The Women's Cancers Section, Laboratory of Molecular Pharmacology (J-CAM, JWC, JN, CEH, DP, PSS) and the Biostatistics and Data Management Section (DJL, SMS), Center for Cancer Research, National Cancer Institute, Bethesda, MD; Institute of Applied Molecular Medicine, Laboratory Animal Science Program, National Cancer Institute, SAIC-Frederick, Frederick, MD (MA); CEU-San Pablo University School of Medicine and Hospital of Madrid Scientific Foundation, Urb. Montepríncipe, Boadilla del Monte, Madrid, Spain (FV-V); Debiopharm S.A., Lausanne, Switzerland (MB, MM); Bristol-Myers Squibb, Pennington, NJ (current affiliation for CEH); Center for Translational Research, Institute for Research and Innovation, Towson, MD (current affiliation for J-CAM).